RSC Advances

PAPER

View Article Online
View Journal | View Issue

Open Access Article. Published on 05 September 2016. Downloaded on 2/7/2026 6:24:04 PM.
This article is licensed under a Creative Commons Attribution-NonCommercial 3.0 Unported Licence.

Cite this: *RSC Adv.*, 2016, **6**, 86269

Amino acid recognition by fine tuning the association constants: tailored naphthalimides in pillar[5]arene-based indicator displacement assays†

Márton Bojtár,[a] Adrien Paudics,[b] Dóra Hessz,[bc] Miklós Kubinyi[bc] and István Bitter*[a]

Received 9th June 2016
Accepted 3rd September 2016

DOI: 10.1039/c6ra15003a

www.rsc.org/advances

Three aminonaphthalimide derivatives were synthesized bearing different anchoring groups in their 4-position in order to adjust the supramolecular interactions with carboxylato-pillar[5]arene (**WP5**), an anionic, water-soluble host. The modification of the anchor groups resulted in varying association constants embracing three orders of magnitude (K_a from $\sim 10^3$ to $\sim 10^6$) in buffered water. Since the fluorophore responded significantly to the electronic environment, large fluorescence quenching was observed with the anionic **WP5** host. The naphthalimide indicator–**WP5** supramolecular assemblies were used to detect arginine and lysine with complete selectivity over other non-basic α-amino acids by turn-on fluorescence. The same assemblies proved to be highly sensitive fluorescence displacement assays for the detection of cadaverine.

Introduction

The construction of fluorescence indicator displacement (FID) assays with macrocyclic receptors is a prosperous field of supramolecular analytical chemistry.[1,2] These systems exploit the principle of competitive binding assays applied extensively in biochemistry: a receptor binds a fluorescent indicator first, creating the sensing assembly, from which the indicator is displaced by the non-fluorescent analyte.[3–5] The fluorescence of the system depends on the concentrations of the bound and free forms of the indicator and thereby on the concentration of the analyte.

Numerous macrocycle–dye complexes were investigated in the past decade applicable as FID assays for the detection of various analytes.[4] The macrocyclic hosts in these complexes were most often cyclodextrins, calixarenes and cucurbiturils.

Pillar[*n*]arenes[6] are a new class of macrocycles, containing *n* hydroquinone units linked together in *p*-position with a methylene bridge. In the past years, various applications were discovered mainly by the versatile host–guest chemistry of these compounds.[7–17] However, these applications were mainly carried out in organic media using primarily alkyl- and functionalised pillararenes. Water soluble pillararenes containing usually ionic (carboxylato-,[18,19] ammonium,[20,21] imidazolium[22] and recently, phosphoryl[23]) groups are emerging as popular hosts in aqueous media. Carboxylato-pillar[*n*]arenes (**WP*n*s**), first synthesized by Ogoshi in 2010 (ref. 18) ($n = 5$) are interesting structures due to their hydrophobic, electron-rich cavity and anionic outer rim. These macrocycles are ideal hosts for ammonium-containing and electron-deficient guests.[18,24–27] As was demonstrated, **WP5** forms strong complexes with basic amino acids and cadaverine, the interactions were, however, monitored only by NMR-studies.[28]

As a first example for a chemosensor, a pillar[5]arene functionalized with a pyrene fluorophore was synthesized by Stoddart to detect diamines in acetonitrile/water mixtures.[29] This was followed by FID assays with **WP*n*** hosts. The operations of a quaternary ammonium attached to tetraphenylethene[30] and an *N*-methylacridinium[31] fluorescent guest in **WP6** and **WP5**, respectively, were demonstrated as FID assays for paraquat. Recently, we reported the complexation of 4-styryl-*N*-methylpyridinium iodide and two other stilbazolium dyes with **WP5** in water[32,33] and proposed a FID system for the colorimetric and fluorescent detection of paraquat with a detection limit of 0.2 μM. To our knowledge, no pillar[5]arene-based indicator displacement assays were constructed for analytes with biological relevance, such as amino acids (AAs).

Detection and quantification of AAs and related compounds is mainly based on chromatographic[34] and electrochemical[35] methods. Besides, in the past years, there has been a rapid progress in the development of fluorescent and colorimetric chemosensors for the detection of AAs,[36] however there is still a need to increase the selectivity and simplicity of these systems. Basic amino acids, arginine (Arg) and lysine (Lys) have *N*-containing units on the side chain that is vital for the proper

[a]*Department of Organic Chemistry and Technology, Budapest University of Technology and Economics, 1521 Budapest, Hungary. E-mail: bitter@oct.bme.hu*

[b]*Department of Physical Chemistry and Materials Science, Budapest University of Technology and Economics, 1521 Budapest, Hungary*

[c]*Institute of Materials and Environmental Chemistry, Research Center for Natural Sciences, Hungarian Academy of Sciences, 1519 Budapest, P. O. B. 286, Hungary*

† Electronic supplementary information (ESI) available. See DOI: 10.1039/c6ra15003a

Open Access Article. Published on 05 September 2016. Downloaded on 2/7/2026 6:24:04 PM.
This article is licensed under a Creative Commons Attribution-NonCommercial 3.0 Unported Licence.

function of the living systems. Their fluorescent and/or colorimetric detection is usually achieved by metal complexes,[37–40] metal nanoparticles,[41–43] cucurbituril- or cucurbituril-analogue-based differential sensing platforms[44–46] or by utilizing their nucleophilicity and basicity for bond cleavage.[47,48] Biogenic diamines are usually detected by non-selective amine chemosensors[49–55] or cucurbituril-based FID systems.[4]

In this paper, our aim has been to introduce a novel principle to construct FID-based chemosensing systems for amino acids. Using an environment-responsive fluorophore attached to different anchors in order to manipulate the association constants, the fine tuning the displacement process is possible to alter sensing parameters (selectivity, sensitivity). This was demonstrated by supramolecular systems containing 4-amino-1,8-naphthalimide fluorophores with three different anchors as guest, and **WP5** as host, the first pillararene-based FID systems to detect basic amino acids. These systems also proved applicable for the detection of biogenic diamines.

Results and discussion

Structures and syntheses

As the fluorophore unit of the guest molecules, the 4-amino-1,8-naphthalimide group was selected, which has the special advantages of convenient derivatization and the easy modulation of its fluorescence *via* photoinduced electron transfer (PET) process.[56] In water, the fluorescence of this fluorophore is quenched due to the stabilization of its ICT state. However, when the substituent attached to the 4-position becomes positively charged, the fluorescence is recovered due to the inhibition of the PET process. This principle is widely used for the fluorescent detection of metal ions.[57–59] Since **WP*n*s** form strong complexes with several cationic guests, such as ammonium, imidazolium and pyridinium compounds, we speculated that some of these groups would be ideal as anchoring moieties.

The expected sensing mechanism of our FID systems is illustrated in Scheme 1. The complexation of the naphthalimide derivatives by **WP5** leads to a fluorescence quenching, since the negative charges on the rim of the pillararene host compensate the positive charge on the anchors of the guests, restoring the PET effect. These systems will then provide a turn-on fluorescence response to the addition of non-fluorescent analytes as competitive guests.

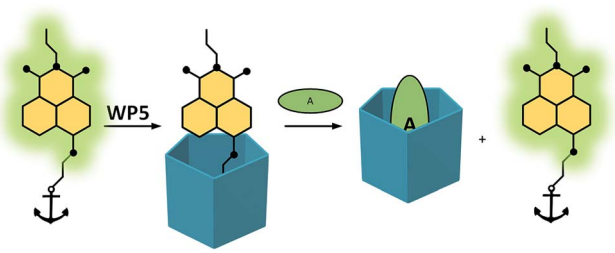

Scheme 1 Anchored naphthalimides in WP5-based indicator displacement systems. The green oval represents the analyte.

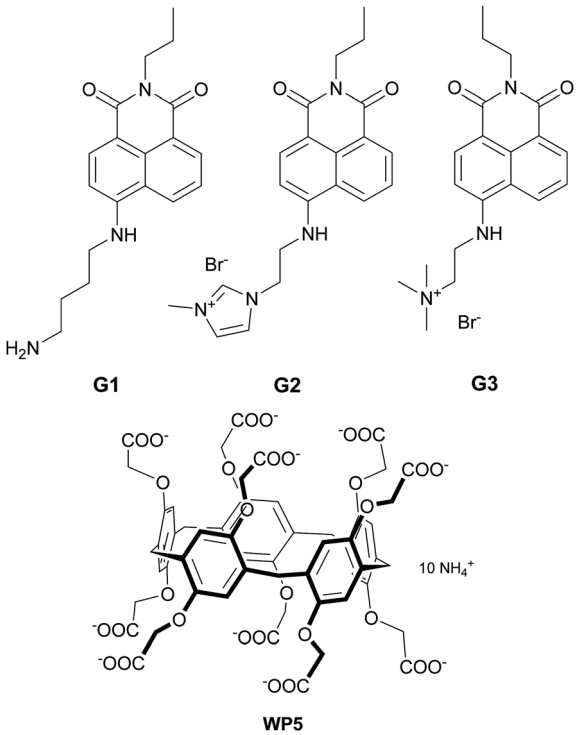

Fig. 1 Structures of the guests **G1–G3** and **WP5**.

Guests **G1–G3** (Fig. 1) were synthesized using the general methods to yield substituted naphthalimides (see ESI for synthetic details†). **WP5** was synthesized as described recently.[60] **G1** has a putrescine anchor and is already mentioned in the literature as an anchored indicator for cucurbituril hosts.[61] **G2** and **G3** are new naphthalimide derivatives. **G2** contains an imidazolium moiety as anchor and was prepared from 4-(2-bromoethylamino)-1,8-naphthalimide[57] and *N*-methylimidazole. **G3** bearing a trimethyl-ammonium end group was synthesized in a similar manner. This latter dye was designed to be a "poorly" complexing indicator since the size of the **WP5** cavity allows only a weaker binding of this guest. The compounds were fully characterised using NMR and HRMS techniques. The complexation studies were performed using optical spectroscopic methods and ^{1}H-NMR measurements.

Complexation studies

As had been expected, all the three guests fluoresced well in HEPES-buffered aqueous media (pH 7.4) due to the inhibition of the PET process by the primary (**G1**) and quaternary (**G2** and **G3**) ammonium anchor groups. The results with the spectral properties are summarized in Table 1. The complexation with the anionic **WP5** caused a significant reduction of the fluorescence due to the charge-compensating effects of the carboxylate arms of the host (Fig. 2). Since the positive charge was effectively shielded, the fluorescence decreased due to the increased PET.

The Job's plots of the indicator–**WP5** systems (ESI Fig. S12–S14†) indicated a stepwise supramolecular reaction: besides the expected 1 : 1 complexes, 2 : 1 (guest : **WP5**) complexes were also formed. The stepwise association constants for the two

 This journal is © The Royal Society of Chemistry 2016

Open Access Article. Published on 05 September 2016. Downloaded on 2/7/2026 6:24:04 PM.
This article is licensed under a Creative Commons Attribution-NonCommercial 3.0 Unported Licence.

Table 1 Spectroscopic data of the naphthalimide guests and their **WP5** complexes

	λ_{abs} (nm)	ε (M^{-1} cm^{-1})	λ_{em} (nm)	Φ
G1	452	14 800	550	0.12
G1·WP5	452	17 600	550	0.02
G2	438	18 800	535	0.20
G2·WP5	437	14 300	535	0.02
G3	434	14 900	533	0.32
G3·WP5	434	14 800	533	0.06

Table 2 Association constants of the complexes

	log K_{a1} (K_{a1} in M^{-1})	log K_{a2} (K_{a2} in M^{-1})
G1·WP5	6.09	6.00
G2·WP5	5.45	5.75
G3·WP5	3.68	—

complexes were determined by a least square fitting to the fluorescence spectra of samples with the same indicator and different **WP5** concentrations (Table 2, see ESI Section 6 for details†). As at the higher **WP5** equivalents, applied in the displacements assays, the dyes were present predominantly in the form of their 1 : 1 **WP5** complexes, the concentrations of 2 : 1 complexes were negligible, we discuss here briefly only the trends in the K_{a1} association constants.

The guests showed the expected variations in complex strength, with K_{a1} values ranging from 10^3 to 10^6 M^{-1}. These results indicate that an efficient supramolecular control could be achieved by the proper selection of the anchoring groups. In the case of **G1**, a strong 1 : 1 complex was formed ($K_{a1,G1} = 1.24 \times 10^6$ M^{-1}) with **WP5**, resulting in an 8-fold reduction of the fluorescence intensity. **G2** also formed an 1 : 1 complex, with a somewhat lower association constant ($K_{a1,G2} = 2.83 \times 10^5$ M^{-1}) and a similar response in fluorescence. The lowest association constant ($K_{a1,G3} = 4.75 \times 10^3$ M^{-1}) was measured in the case of **G3**. This demonstrates that the trimethylammonium group functions as a "poorly complexing" anchor.

The supramolecular interactions in the complexes were further evaluated using ^{1}H-NMR measurements in D_2O (Fig. 3). The complexation was fast enough to present one set of signals in each case. In the case of **G1**, the protons of the anchor moiety displayed unusually large upfield shifts (up to $\Delta\delta = -3.4$ ppm) making some of the methylene protons appear at negative chemical shifts. The aromatic protons of the fluorophore showed slight downfield shifts with the exception in the 3-position near the anchor unit that exhibited some upfield shift. This can be rationalized by the partial inclusion of the molecule illustrated in Scheme 1: the anchoring unit penetrates the cavity, whereas the naphthalimide moiety remains at the rim of the macrocycle. The protons of the host remained mostly unchanged, which indicates that there was no significant restriction in the movement of the constituent units. Similar effects were observed with **G2**: large upfield shifts of the *N*-methylimidazolium protons (up to $\Delta\delta = -1.1$ ppm) and the spacer methylene units (up to $\Delta\delta = -2.4$ ppm) accompanied by the broadening of the signals, which is attributable to the shielding effect of the macrocycle. The aromatic protons of **G2** exhibited some downfield shifts as well. Due to the positive charge on the **G2** guest, some changes could be detected in the signals of the **WP5** macrocyclic host. The sterically less favorable guest **G3** showed somewhat different changes: we suppose that due to steric hindering, complete inclusion could not be reached, therefore only small changes were detected in the signals of the anchor moiety (*i.e.* the trimethylammonium group showed $\Delta\delta = -0.13$ ppm). The different complexation was also suggested by the upfield shifts of the aromatic protons of the naphthalimide unit.

To gain further insight into these distinct host–guest interactions, we calculated the anchor volumes and compared them to the cavity volume of pillar[5]arene. It was confirmed that the ethylammonium ion (anchor for **G1**) with a volume of 77 Å^3, and the *N*,*N*′-ethyl-methyl imidazolium cation (anchor for **G2**) filling a volume of 143 Å^3 can be included in the 152 Å^3 cavity of the **WP5** pillarene host,[9] whereas the volume of *N*,*N*-ethyl-trimethylammonium moiety (anchor for **G3**) is 171 Å^3, exceeds the above cavity volume of **WP5**, preventing such type host–guest interaction (see ESI Section 7 for details†).

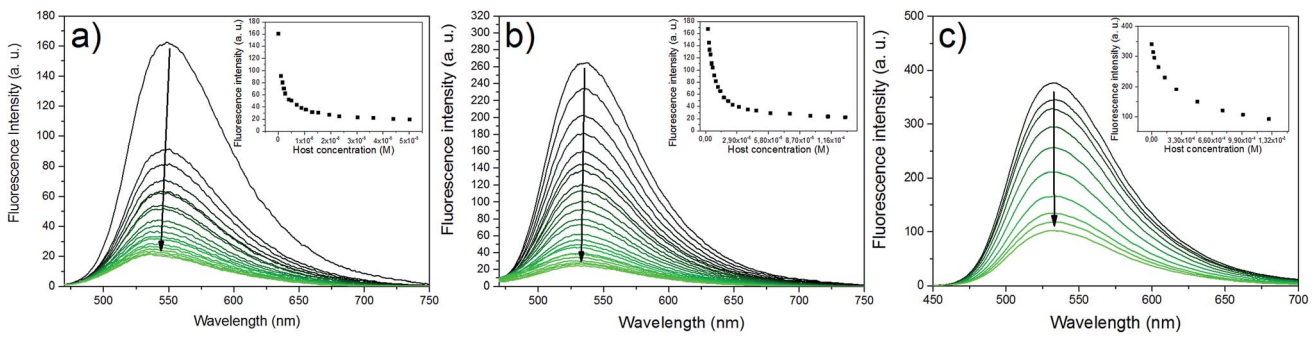

Fig. 2 Fluorescence titration of the guests with **WP5** in HEPES buffer (pH 7.4). In each case, the concentration of the indicators was 1 μM. (a) **G1** + **WP5** (0 to 50 equivalent), excitation at 450 nm; (b) **G2** + **WP5** (0 to 128 equivalent), excitation at 399 nm; (c) **G3** + **WP5** (0 to 1280 equivalent), excitation at 433 nm; the insets show the fluorescence emission *vs.* host concentration at 550 nm.

Open Access Article. Published on 05 September 2016. Downloaded on 2/7/2026 6:24:04 PM.
This article is licensed under a Creative Commons Attribution-NonCommercial 3.0 Unported Licence.

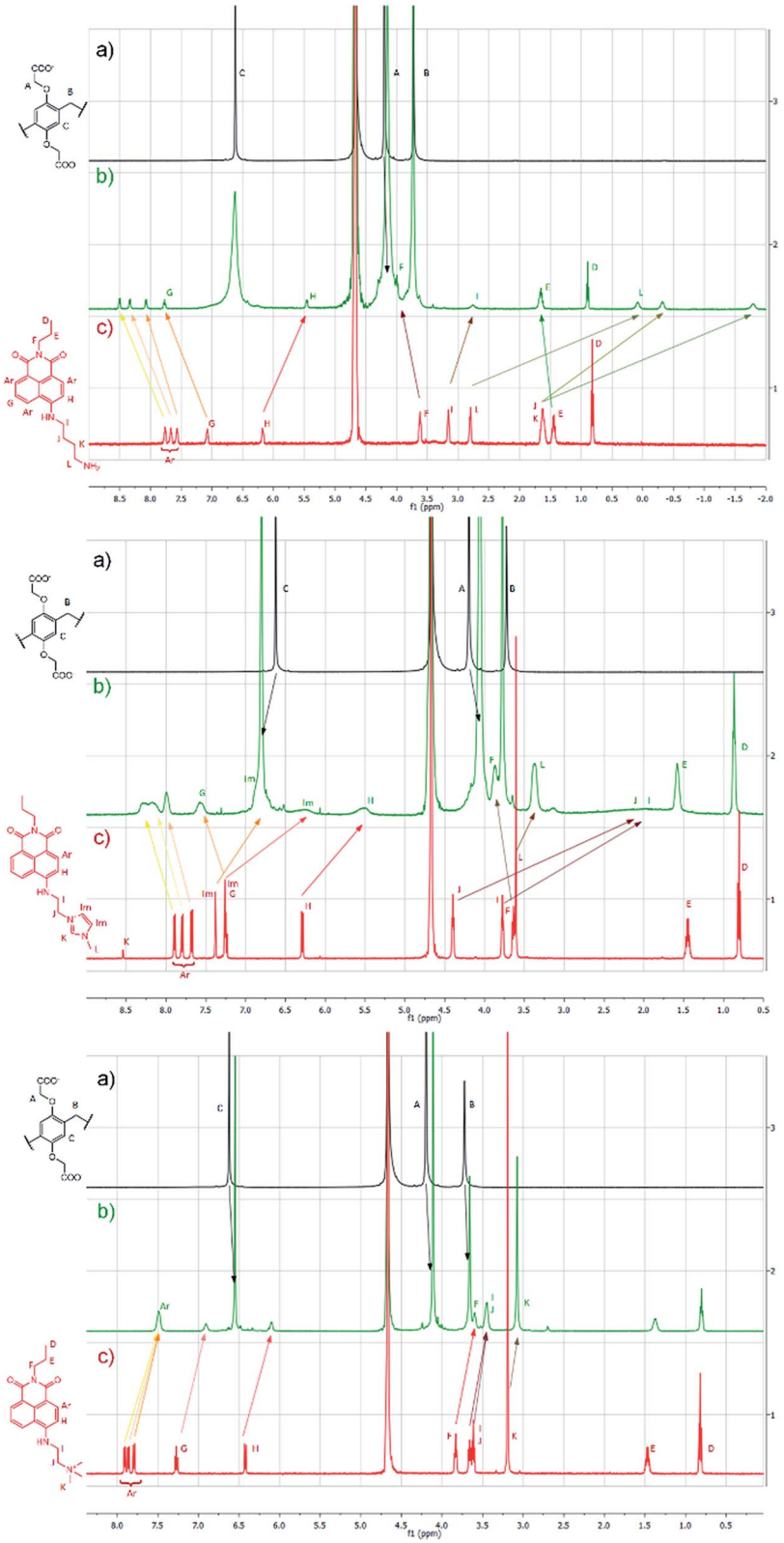

Fig. 3 ^{1}H-NMR spectra (500 MHz, 25 °C) of the guests **G1–G3** (a) **WP5** (b) **Gx·WP5** (c) **Gx** in D_2O maintaining a constant concentration of 3 mM for all components.

Fluorescence indicator displacement

Due to their large signal modulation upon complexation and optimal binding constants with **WP5**, **G1** and **G2** were selected as potential indicators for FID systems. Upon addition of various amino acids (3 mM) to the indicator–**WP5** complexes, a significant fluorescence enhancement was observed only in

 This journal is © The Royal Society of Chemistry 2016

Open Access Article. Published on 05 September 2016. Downloaded on 2/7/2026 6:24:04 PM.
This article is licensed under a Creative Commons Attribution-NonCommercial 3.0 Unported Licence.

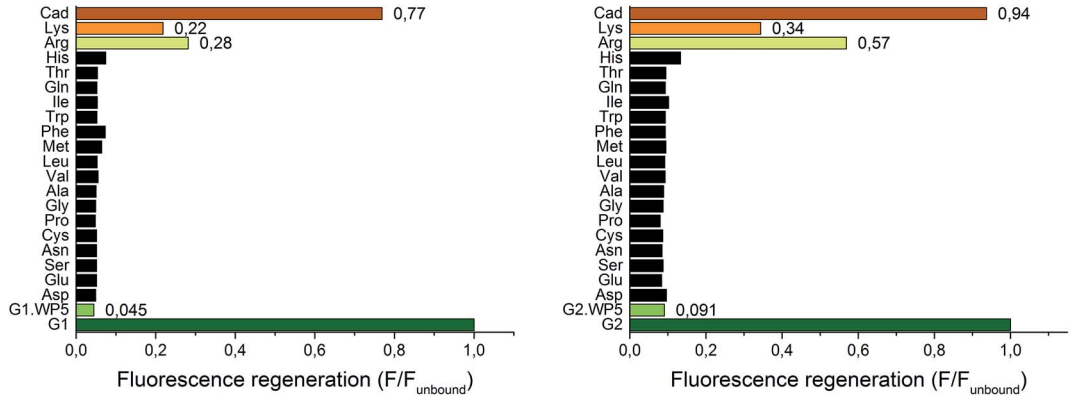

Fig. 4 Fluorescence regeneration values ($F/F_{unbound}$) at 550 nm of cadaverine (Cad) and various amino acids using **G1·WP5** (left, excitation at 450 nm) and **G2·WP5** (right, excitation at 399 nm) systems as indicator displacement assays. For the screening experiments, the concentrations of the indicators were 3 μM using 15 equivalent host. The analytes were added in 3 mM concentration.

the cases of arginine and lysine. The effect could be characterized by the fluorescence regeneration, $F/F_{unbound}$, which is related to the proportion of the displaced indicators (Fig. 4).

The screening experiment showed that the addition of non-basic α-amino acids in high concentration caused negligible changes in the fluorescence, with the exception of histidine, which resulted in a small fluorescence enhancement. Thus, both of our FID systems showed a high selectivity towards the basic amino-acids. The two diamines, putrescine and cadaverine caused an almost complete fluorescence regeneration of the free indicators (only cadaverine shown). Subsequently, titration experiments were performed to evaluate the sensitivity of the two indicator displacement systems for cadaverine, arginine and lysine (Fig. S15 and S16†). A host concentration of 15 μM was selected (15-fold excess related to the indicator guest) to achieve a high level of indicator–**WP5** complex, which was ~95% for the **G1·WP5** and ~80% for the **G2·WP5** system as can be calculated from the respective K_a values.

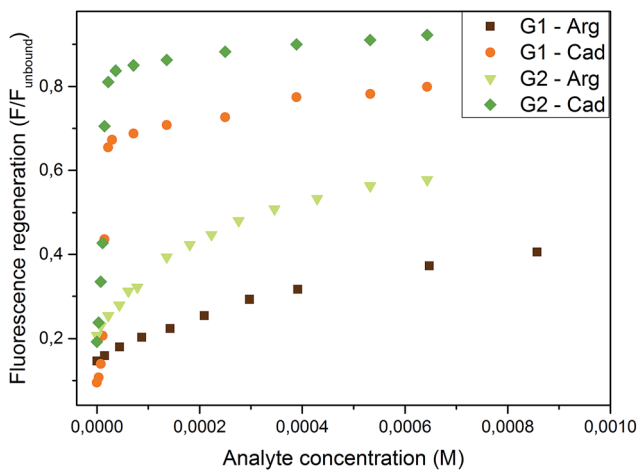

Fig. 5 Fluorescence regeneration ($F/F_{unbound}$) of indicators **G1** and **G2** at 550 nm, caused by their displacements from their **WP5** complexes by arginine and cadaverine. In this case, 1 μM indicator concentration and 15 equivalent of host were used.

Both systems were found highly sensitive for cadaverine with a large turn-on fluorescence. A smaller, but still significant enhancement was induced by arginine and an even smaller enhancement was reached with lysine. The weaker **G2·WP5** complex showed the expected higher sensitivity towards the analytes, as can be seen in Fig. 5. The limit of detection (LOD; for its calculation see ESI Section 8†) was found to be larger by almost one order of magnitude in the case of **G2·WP5**: for cadaverine, the LOD was found to be 9.44×10^{-7} M and 1.41×10^{-7} M for **G1·WP5** and **G2·WP5**, respectively. In the case of arginine, the LOD value of 1.34×10^{-5} M was obtained for the **G1·WP5** assay and 3.27×10^{-6} M for the **G2·WP5** assay. This example demonstrates that the sensing properties can be tailored and fine-tuned with varying the anchor unit with the same fluorophore. In addition, due to the different sensitivity of these systems, differential sensing can be achieved based on the anchored naphthalimide indicators and **WP5**.

The indicator displacement was further evaluated by ^{1}H-NMR-spectroscopy. Following the NMR investigation of the naphthalimide–**WP5** mixtures (see Section 'Complexation studies'), the mixtures of the guests with cadaverine and arginine were tested in the absence of the host (Fig S17–S20†). No significant changes were observed showing the lack of interaction of the indicators with the analytes. In the case of **G1**, the slight shift of the signals could be attributed to the pH sensitivity of the anchor group. Next, the indicator displacement process was studied by NMR spectroscopy (Fig. S21–S24†). Upon addition of cadaverine in 10-fold excess to the complexes of **WP5** with **G1** and **G2**, the displacement of the indicators was clearly visible, as the spectra of the free indicators were regained. However, when arginine was added to the **G1·WP5** complex in the same excess, an average signal of the complex and the free **G2** was observed as a result of partial displacement. Unfortunately, upon the addition of arginine to **G1·WP5** precipitation occurred, it is unlikely, however, that in the latter system the indicator was displaced from the strong complex.

With respect to the acid–base character of components, some aspects of the pH-dependence of the complexation and displacement reactions were also investigated. As could be

Open Access Article. Published on 05 September 2016. Downloaded on 2/7/2026 6:24:04 PM.
This article is licensed under a Creative Commons Attribution-NonCommercial 3.0 Unported Licence.

expected, the complexation of **G1** was pH-dependent (ESI Section 10†), however, the association constants for **G2·WP5** were almost identical in the 6.8–8.2 pH range. The indicator displacement of **G2·WP5** was tested at pH values 6.8, 7.4 and 8.2: evidently, higher fluorescence regeneration values were detected for the basic amino acids at lower pH, whereas, for cadaverine, no correlation was found (Fig. S25†).

As a further test of the **G2·WP5** system, the more sensitive FID sensor for basic amino acids, the association constants for the lysine–**WP5** and arginine–**WP5** supramolecular complexes were determined by a least square fitting to the fluorescence spectra of **G2·WP5**–lysine/arginine mixtures, with different lysine/arginine concentrations. For the lysine–**WP5** complex $K_a = 1.12 \times 10^3\ M^{-1}$ was obtained, for the arginine–**WP5** complex $K_a = 5.24 \times 10^3\ M^{-1}$, in good agreement with the values of $1.8 \times 10^3\ M^{-1}$ for lysine–**WP5** and $5.9 \times 10^3\ M^{-1}$ for arginine–**WP5** determined by NMR experiments.[28]

Conclusions

In conclusion, the synthesized 4-amino-1,8-naphthalimide indicators having different anchoring groups in the 4-position were shown to form complexes with **WP5** with varying association constants and large signal modulation. Two complexes were tested as indicator displacement systems for cadaverine, putrescine and α-amino acids. Both systems can detect cadaverine and the basic amino acids with high selectivity and different sensitivity. The FID process was further established using NMR spectroscopy. To our knowledge, this is the first **WP5**-based FID sensing system for analytes with biological relevance. We believe that the current toolbox of indicator displacement assays could be further expanded with this intriguing host.

Acknowledgements

We thank the Hungarian Research Foundation for the financial support of this work (Grant No. K108752). We are grateful to Fanni Bazsó for the mass spectrometric measurements and Zoltán Szakács for the anchor volume calculations.

Notes and references

1 E. V. Anslyn, *J. Org. Chem.*, 2007, **72**, 687–699.
2 L. You, D. Zha and E. V. Anslyn, *Chem. Rev.*, 2015, **115**, 7840–7892.
3 B. T. Nguyen and E. V. Anslyn, *Coord. Chem. Rev.*, 2006, **250**, 3118–3127.
4 R. N. Dsouza, U. Pischel and W. M. Nau, *Chem. Rev.*, 2011, **111**, 7941–7980.
5 G. Ghale and W. M. Nau, *Acc. Chem. Res.*, 2014, **47**, 2150–2159.
6 T. Ogoshi, S. Kanai, S. Fujinami, T.-a. Yamagishi and Y. Nakamoto, *J. Am. Chem. Soc.*, 2008, **130**, 5022–5023.
7 P. J. Cragg and K. Sharma, *Chem. Soc. Rev.*, 2012, **41**, 597–607.
8 T. Ogoshi, *J. Inclusion Phenom. Macrocyclic Chem.*, 2012, **72**, 247–262.
9 M. Xue, Y. Yang, X. Chi, Z. Zhang and F. Huang, *Acc. Chem. Res.*, 2012, **45**, 1294–1308.
10 T. Ogoshi and T.-a. Yamagishi, *Eur. J. Org. Chem.*, 2013, **2013**, 2961–2975.
11 H. Zhang and Y. Zhao, *Chem.–Eur. J.*, 2013, **19**, 16862–16879.
12 D. Cao and H. Meier, *Asian J. Org. Chem.*, 2014, **3**, 244–262.
13 C. Li, *Chem. Commun.*, 2014, **50**, 12420–12433.
14 D. Cao and H. Meier, *Synthesis*, 2015, **26**, 1041–1056.
15 K. Yang, Y. Pei, J. Wen and Z. Pei, *Chem. Commun.*, 2016, **52**, 9316–9326.
16 T. Ogoshi, T. A. Yamagishi and Y. Nakamoto, *Chem. Rev.*, 2016, **116**, 7937–8002.
17 Y. Wang, G. Ping and C. Li, *Chem. Commun.*, 2016, **52**, 9858–9872.
18 T. Ogoshi, M. Hashizume, T.-a. Yamagishi and Y. Nakamoto, *Chem. Commun.*, 2010, **46**, 3708–3710.
19 G. Yu, M. Xue, Z. Zhang, J. Li, C. Han and F. Huang, *J. Am. Chem. Soc.*, 2012, **134**, 13248–13251.
20 Y. Ma, X. Ji, F. Xiang, X. Chi, C. Han, J. He, Z. Abliz, W. Chen and F. Huang, *Chem. Commun.*, 2011, **47**, 12340–12342.
21 G. C. Yu, J. Zhou, J. Shen, G. P. Tang and F. H. Huang, *Chem. Sci.*, 2016, **7**, 4073–4078.
22 Y. Yao, J. Li, J. Dai, X. Chi and M. Xue, *RSC Adv.*, 2014, **4**, 9039–9043.
23 W. Cheng, H. Tang, R. Wang, L. Wang, H. Meier and D. Cao, *Chem. Commun.*, 2016, **52**, 8075–8078.
24 C. Li, X. Shu, J. Li, S. Chen, K. Han, M. Xu, B. Hu, Y. Yu and X. Jia, *J. Org. Chem.*, 2011, **76**, 8458–8465.
25 S. Dasgupta, A. Chowdhury and P. S. Mukherjee, *RSC Adv.*, 2015, **5**, 85791–85798.
26 B. Shi, K. Jie, Y. Zhou, J. Zhou, D. Xia and F. Huang, *J. Am. Chem. Soc.*, 2016, **138**, 80–83.
27 Y. Sun, F. Guo, T. Zuo, J. Hua and G. Diao, *Nat. Commun.*, 2016, **7**, 12042.
28 C. Li, J. Ma, L. Zhao, Y. Zhang, Y. Yu, X. Shu, J. Li and X. Jia, *Chem. Commun.*, 2013, **49**, 1924–1926.
29 N. L. Strutt, R. S. Forgan, J. M. Spruell, Y. Y. Botros and J. F. Stoddart, *J. Am. Chem. Soc.*, 2011, **133**, 5668–5671.
30 P. Wang, X. Yan and F. Huang, *Chem. Commun.*, 2014, **50**, 5017–5019.
31 P. Wang, Y. Yao and M. Xue, *Chem. Commun.*, 2014, **50**, 5064–5067.
32 M. Bojtar, Z. Szakacs, D. Hessz, M. Kubinyi and I. Bitter, *RSC Adv.*, 2015, **5**, 26504–26508.
33 M. Bojtár, Z. Szakács, D. Hessz, F. L. Bazsó, M. Kállay, M. Kubinyi and I. Bitter, *Dyes Pigm.*, 2016, **133**, 415–423.
34 J. Le Boucher, C. Charret, C. Coudray-Lucas, J. Giboudeau and L. Cynober, *Clin. Chem.*, 1997, **43**, 1421–1428.
35 G. L. Luque, N. F. Ferreyra and G. A. Rivas, *Talanta*, 2007, **71**, 1282–1287.
36 Y. Zhou and J. Yoon, *Chem. Soc. Rev.*, 2012, **41**, 52–67.
37 A. Buryak and K. Severin, *J. Am. Chem. Soc.*, 2005, **127**, 3700–3701.
38 X. Zhou, X. Jin, D. Li and X. Wu, *Chem. Commun.*, 2011, **47**, 3921–3923.
39 L. He, V. L. L. So and J. H. Xin, *Sens. Actuators, B*, 2014, **192**, 496–502.

 This journal is © The Royal Society of Chemistry 2016

Open Access Article. Published on 05 September 2016. Downloaded on 2/7/2026 6:24:04 PM.
This article is licensed under a Creative Commons Attribution-NonCommercial 3.0 Unported Licence.

40 J. Cao, L. Ding, Y. Zhang, S. Wang and Y. Fang, *J. Photochem. Photobiol., A*, 2016, **314**, 66–74.
41 D. Xiong, M. Chen and H. Li, *Chem. Commun.*, 2008, 880–882, DOI: 10.1039/B716270G.
42 G. Patel and S. Menon, *Chem. Commun.*, 2009, 3563–3565, DOI: 10.1039/B905141D.
43 K. A. Rawat and S. K. Kailasa, *Microchim. Acta*, 2014, **181**, 1917–1929.
44 D. M. Bailey, A. Hennig, V. D. Uzunova and W. M. Nau, *Chem.–Eur. J.*, 2008, **14**, 6069–6077.
45 L. A. Baumes, M. Buaki, J. Jolly, A. Corma and H. Garcia, *Tetrahedron Lett.*, 2011, **52**, 1418–1421.
46 T. Minami, N. A. Esipenko, B. Zhang, L. Isaacs and P. Anzenbacher, *Chem. Commun.*, 2014, **50**, 61–63.
47 X. Lu, W. Wang, Q. Dong, X. Bao, X. Lin, W. Zhang, X. Dong and W. Zhao, *Chem. Commun.*, 2015, **51**, 1498–1501.
48 X. Qian, W. Gong, F. Wang, Y. Lin and G. Ning, *Tetrahedron Lett.*, 2015, **56**, 2764–2767.
49 K. Secor, J. Plante, C. Avetta and T. Glass, *J. Mater. Chem.*, 2005, **15**, 4073–4077.
50 G. Lu, J. E. Grossman and J. B. Lambert, *J. Org. Chem.*, 2006, **71**, 1769–1776.
51 S. Reinert and G. J. Mohr, *Chem. Commun.*, 2008, 2272–2274, DOI: 10.1039/B717796H.
52 M.-S. Steiner, R. J. Meier, A. Duerkop and O. S. Wolfbeis, *Anal. Chem.*, 2010, **82**, 8402–8405.
53 B. Lee, R. Scopelliti and K. Severin, *Chem. Commun.*, 2011, **47**, 9639–9641.
54 J.-F. Lin, J. Kukkola, T. Sipola, D. Raut, A. Samikannu, J.-P. Mikkola, M. Mohl, G. Toth, W.-F. Su, T. Laurila and K. Kordas, *J. Mater. Chem. A*, 2015, **3**, 4687–4694.
55 Y. Hu, X. Ma, Y. Zhang, Y. Che and J. Zhao, *ACS Sens.*, 2016, **1**, 22–25.
56 R. M. Duke, E. B. Veale, F. M. Pfeffer, P. E. Kruger and T. Gunnlaugsson, *Chem. Soc. Rev.*, 2010, **39**, 3936–3953.
57 T. Chen, W. Zhu, Y. Xu, S. Zhang, X. Zhang and X. Qian, *Dalton Trans.*, 2010, 1316–1320.
58 G. R. C. Hamilton, S. K. Sahoo, S. Kamila, N. Singh, N. Kaur, B. W. Hyland and J. F. Callan, *Chem. Soc. Rev.*, 2015, **44**, 4415–4432.
59 J. Yin, Y. Hu and J. Yoon, *Chem. Soc. Rev.*, 2015, **44**, 4619–4644.
60 R. R. Kothur, J. Hall, B. A. Patel, C. L. Leong, M. G. Boutelle and P. J. Cragg, *Chem. Commun.*, 2014, **50**, 852–854.
61 C. P. Carvalho, R. Ferreira, J. P. Da Silva and U. Pischel, *Supramol. Chem.*, 2013, **25**, 92–100.